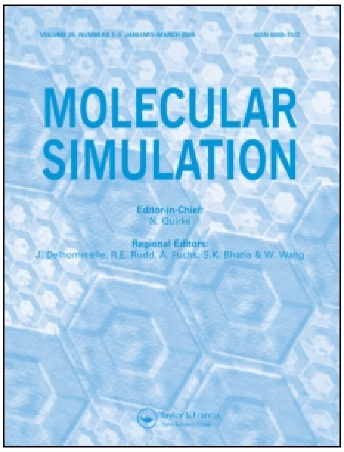

Molecular Simulation
Publication details, including instructions for authors and subscription information:
http://www.informaworld.com/smpp/title~content=t713644482

Performance of rigid water models in the phase transition of clathrates†

D. P. Luis[a]; J. López-Lemus[a]; M. Mayorga[a]; L. Romero-Salazar[a]
[a] Facultad de Ciencias, Universidad Autónoma del Estado de México, Toluca, CP 50000, Mexico

To cite this Article Luis, D. P. , López-Lemus, J. , Mayorga, M. and Romero-Salazar, L.(2010) 'Performance of rigid water models in the phase transition of clathrates†', Molecular Simulation, 36: 1, 35 — 40, First published on: 26 August 2009 (iFirst)

To link to this Article: DOI: 10.1080/08927020903096072

URL: http://dx.doi.org/10.1080/08927020903096072

Molecular Simulation
Vol. 36, No. 1, January 2010, 35–40

Performance of rigid water models in the phase transition of clathrates[†]

D.P. Luis[1], J. López-Lemus*, M. Mayorga[2] and L. Romero-Salazar[3]

Facultad de Ciencias, Universidad Autónoma del Estado de México, Av. Instituto Literario 100, CP 50000 Toluca, Mexico

(*Received 3 April 2009; final version received 2 July 2009*)

Molecular dynamic simulations in the NPT ensemble were performed to analyse the structural properties of methane hydrate by using rigid water models of three, four and five sites (SPC/E, TIP4P and TIP5P). An exploratory study was carried out concerning the capabilities of these water models in the near region of the phase transition line (pressure–temperature). This task was achieved by performing simulations at a constant pressure of 20 atm, varying the temperature from 200 to 300 K. The radial distribution function as well as the coordination number for carbon and oxygen sites were obtained for the above-mentioned temperatures: both of them allow us to observe the stable–unstable phase transition of the methane hydrate. As a result, we can mention that the structural properties estimated with the three sites water model show an excellent agreement with the experimental results, specifically around the phase transition line. In addition, the coordination number becomes a useful criterion to demonstrate the dissociation of the clathrates. On the other hand, the potential of mean force between two methane molecules in water is shown in the same vicinity, evidencing the energetic cost to keep the clathrate in a stable thermodynamic state.

Keywords: methane hydrate; water mode; coordination number; potential of mean force; radial distribution function

PACS: 31.15.Qg; 61.20.Ja

1. Introduction

Natural gas hydrates are non-stoichiometric inclusion compounds in which water molecules form cavities or cages. These cavities consist of a crystalline host lattice (structural arrangements of water molecules) that trap gas molecules called guest molecules. The solid structure conformed just by water is thermodynamically unstable at low temperatures and moderate high pressures. Also, due to the presence of the guest species, the empty clathrate becomes stabilised. According to the experimental evidence, the cages are big enough to allocate guest molecules and they are supported by the effect of the hydrogen bonds of water molecules [1,2]. Different kinds of gas hydrate structures can be obtained depending on the nature of the guest, but the most important crystalline structures are identified as: sI, sII and sH [2]. On the other hand, by means of X-ray scattering, it is possible to determine the structure of this kind of compound. Type sI, the one in which we are interested, is formed by six cavities called pentagonal dodecahedrons and denoted by 5^{12} (a polyhedron formed by 12 pentagonal faces) and two cavities called tetracadecahedron $5^{12}6^2$ (a polyhedron formed by 12 pentagonal faces and two hexagonal faces) [3]. In this unit cell, there are 46 water molecules and the number of gas molecules may vary, eight being the number of molecules for which all cavities of the cell are occupied.

In the literature, it is often mentioned that a non-polar molecule surrounded by water shows the hydrophobicity phenomena [4,5]. In some works, the potential of mean force (PMF) [6] has been employed to analyse the hydrophobic interaction [7–10], where two minima can be observed, one of them corresponds to the contact configuration and the other one corresponds to the solvent-separated configuration. For example, this function allows us to observe the energy barrier that the water molecules have to overcome in order to hydrate a methane molecule, in particular. Pratt and Chandler [4] have shown that the second minimum is more probable than the first one for two hard spheres. They argue that an entropic driving force induces the approach between pairs of hard spheres. Recently, Wynveen and Bresme [11] have studied the interactions of polarisable solutes in water as a function of the solute permittivity (ϵ). They state that the hydrophobic interactions among solutes strongly depend on the permittivity values of the solute ϵ. Their argument is that, for low permittivity, the interactions are dominated by surface tension forces whose origin lies in the formation of a vapour cavity between the two hydrophobic solutes. All this information helps to establish that, by changing the polar nature of the solute, it is possible to observe an increment or decrement in the hydrophobic effect. Haymet put forward another point of view [12]. He suggested that water is

---

[†] In memory of our friend, Yurko Duda.
*Corresponding author. Email: jllemus@uaemex.mx

ISSN 0892-7022 print/ISSN 1029-0435 online

DOI: 10.1080/08927020903096072
http://www.informaworld.com

methophobic, i.e. methane has an affinity for water and not vice versa. This kind of molecule at specific thermodynamic conditions (low temperature and moderate high pressure) shows a special structural arrangement. As has already been mentioned, the presence of the guest molecules stabilises the system, but also the hydrophobic interaction between the water and its guest molecules could recover importance as the pressure is increased. The latter has been discussed by Hummer et al. [10]. They argue that at low pressures the water molecules cannot occupy the interstitial space between two non-polar molecules because it is energetically unfavourable. The opposite situation takes place as the pressure increases; hence, the solvent-separated configuration is more relevant compared to the contact pairing.

The sI structure of methane hydrate has been observed in experiments [13,14] and reproduced by computer simulations [15,16]. There are some efforts to study the structure of clathrate by molecular simulation, where the hydrophobic phenomenon is present [16] and more than one water model has been used. Some of these results supported by computer simulations have been developed in the stable regimen of clathrate; however, we are interested in analysing the structural changes of methane hydrate under an external electric field, in the region where the stable–unstable transition of methane hydrate is experimentally located. However, there is a step that must be overcome first; a water model must be chosen that works in the transition line; in other words, we would like to select a model that reproduces the experimental evidence of the clathrate dissociation when the temperature increases [17]. This strengthens the importance of the water model for an analysis at a molecular level [18]. Hence, the purpose of the present study is to apply molecular dynamics to compare the performance of rigid water models of three, four and five sites in the estimation of structural properties of methane hydrate, in the vicinity of the phase transition [19]. In this paper, the radial distribution function (RDF) [20,21] for different atom pairs and the coordination number between carbon and oxygen atoms were calculated, varying the temperature and maintaining always the pressure constant. When the stable methane hydrates are located under the influence of high temperatures, the experimental evidence indicates that such systems begin to be destabilised; thus with the purpose of having a clear idea of this structural changes, the mean force potential between each two methane atoms is estimated. The present work is organised as follows. In Section 2, some details of the molecular simulation are mentioned. In Section 3, relevant results are included as well as a brief discussion about them. Finally, some conclusions from this work are contained in Section 4.

2. Methodology

We have performed simulations of the methane hydrates by using different water models in an NPT ensemble. In this work, we have used three rigid non-polarisable models of water: SPC/E [22], TIP4P [23] and TIP5P [24]. The methane molecule is also modelled as a rigid molecule [25], consisting of five sites with a contribution of van der Waals interaction modelled by Lennard-Jones potential in the carbon atoms. Partial charges were assigned to both kinds of atoms, i.e. carbon and hydrogen. The link C—H and the linking angle H—C—H were set 1.09 and 109.47 Å, respectively. The Lorentz–Berthelot combining rules were employed between different kinds of atoms. It was decided to restrict this paper to the study of the rigid models of water of three, four and five sites, as a starting point due to their simplicity when they are implemented. The simulations were developed using a modified version of the TINKER program; they were performed using periodic boundary conditions and the minima image convention in the three directions. The Ewald sums method was used to estimate the long-range interactions of the charge particles, in fact, this method is an excellent option to estimate the long range interaction for both polar and non-polar potentials [18,26–29]. The chosen cut-off radius was of $R_c = 11$ Å and rigid body algorithm [30] was used for estimating the evolution of the molecules in space and time, keeping the pressure by means of the Berendsen barostat [31].

The initial configuration for the simulations was based on the X-ray results obtained by McMullan and Jeffrey [32] for the type I structure of the ethylene oxide hydrate, which provides the positions of the oxygen atoms in every water molecule and the mass centres in the unit cell for the methane molecules. The orientations of the hydrogen atoms in the water molecules were set randomly. The unit cell of side $L_x = L_y = L_z = 12.03$Å at 25°C was replicated $2 \times 2 \times 2$ times to form a cubic cell of side 24.06 Å, which includes 368 water molecules and 64 methane molecules; this means that the 'cages' formed by water in methane hydrates are completely occupied. This initial configuration was balanced for 50 ps at $T = 50$ K and $P = 1$ atm to correctly orientate the hydrogen atoms of the water molecules. This procedure was done in order to create the cages, which constitute the initial configuration in all our simulations. All the simulations were developed at 20 atm. The temperature was chosen from a long range: 200, 220, 240, 260, 280, 290 and 300 K, which implies that the equilibrium experimental line was crossed in the phase diagram of the methane hydrates. Actually for the particular pressure 20 atm, the experimental temperature of transition is located at 265–275 K [17].

For the determination of the effective coordination number [6], the following relation was used:

$$n = 4\pi n \int_0^{r_{\mathrm{ref}}} r^2 g(r)\,\mathrm{d}r, \qquad (1)$$

where $g(r)$ is the RDF [20,21] and n is the number of water molecules. The integral is over the first shell of coordination which ends at r_{ref}, for each graphic.

Since the PMF, $W(r)$, is the free energy required to put together a pair of atoms at a distance r, bringing them from infinity, it can be written in terms of the RDF as follows:

$$W(r) = -K_B T \ln g_{ij}(r), \tag{2}$$

where r is the distance of separation, K_B is Boltzmann's constant and g_{ij} is the RDF for two kinds of atoms, i and j.

3. Results and discussion

In this section, the relevant results of this work are shown. By means of molecular dynamics, the methane hydrates were simulated under specific thermodynamic conditions. The starting point is to consider the methane hydrate already formed and located in a stable state, and then by varying the temperature the structural changes are analysed for three different water models. These structural modifications are captured using the RDF of the methane hydrate.

In Figure 1, a snapshot of the clathrate is shown at a stable thermodynamic state, temperature 200 K and pressure 20 atm. This figure mimics the structural status of the compounds where the methane is trapped by water cages. In Figure 2, the carbon–oxygen RDF for clathrate is shown for three different water models at temperature 200 K and pressure 20 atm. From this figure, we can see that the three water models show a stable system. In Figure 3, the carbon–carbon RDF for clathrate is shown in the same thermodynamic state for the three water models. The RDFs obtained by using these water models (Figures 2 and 3) are very similar to those in figures 4 and 6 of [16], respectively. The carbon–oxygen RDF for the three water models used here is estimated at 20 atm for different temperatures; these results are presented in Figures 4 (SPC/E), 5 (TIP4P) and 6 (TIP5P). These curves were obtained from a series of simulations varying the temperature from $T = 200$ to 300 K. These temperatures cross the equilibrium line in the phase diagram of the methane hydrates [17]. Figure 4 corresponds to a clathrate

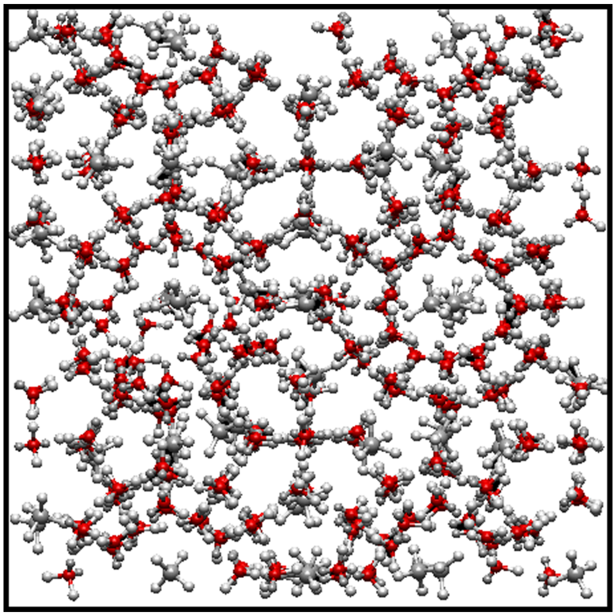

Figure 1. Snapshot of a clathrate at 20 atm and 200 K. The methane compounds are located in a stable thermodynamic state. The five sites methane molecule model was used for this simulation and this kind of molecule can be observed surrounded by water molecules forming cages.

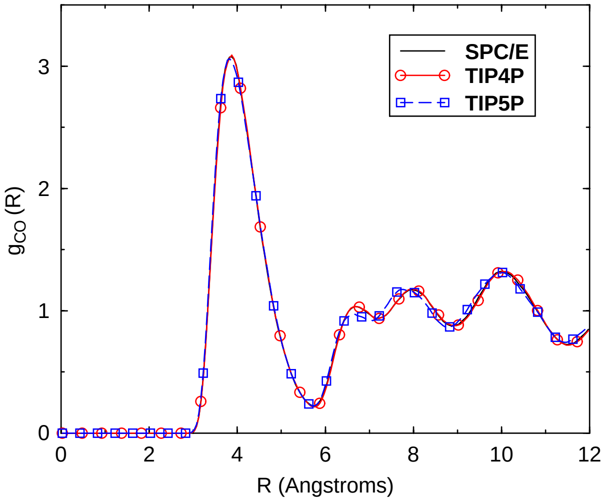

Figure 2. RDF of carbon–oxygen at 20 atm and 200 K. Three different water models were used. The continuous line without symbols corresponds to the SPC/E water model results, the empty circles and squares are data from the TIP4P and TIP5P water models, respectively. These curves are similar among them and they basically show a stable methane hydrate; see [16].

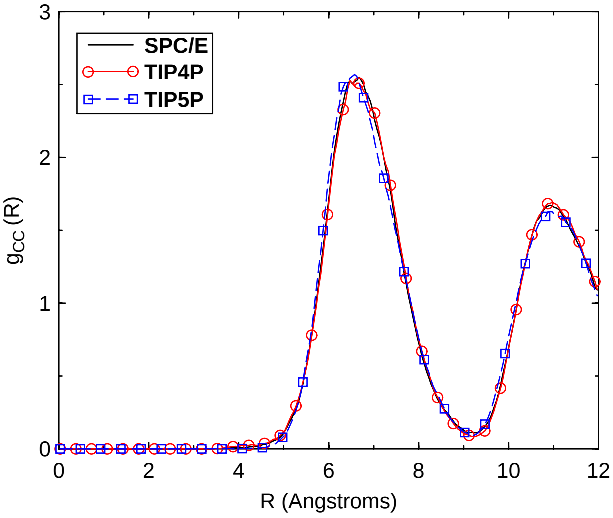

Figure 3. RDF of carbon–carbon at 20 atm and 200 K. For all different water models used in this work. The stable state is reached by the three water models.

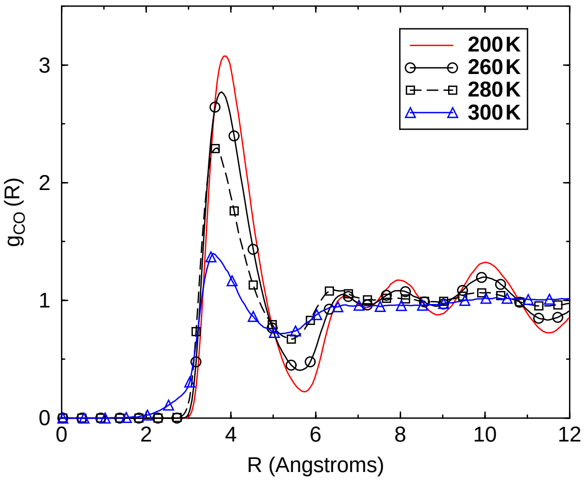

Figure 4. RDF of carbon–oxygen at 20 atm but varying the temperature from $T = 200$ to 300 K. The SPC/E water model was employed for these curves. The spacial order is affected by the increase of temperature.

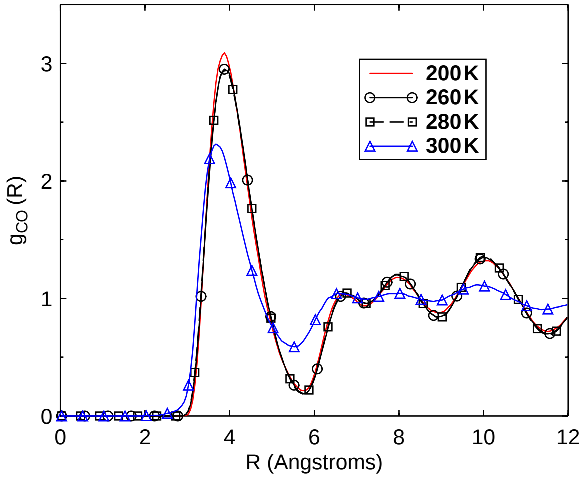

Figure 5. RDF of carbon–oxygen at 20 atm, varying the temperature from $T = 200$ to 300 K. In this graph, the TIP4P water model was used. The structural changes are less known for this water model when the temperature is increased.

simulation using the SPC/E water model. In Figure 5, the TIP4P water model was used and in Figure 6 the TIP5P water model was applied in the simulation. As it is well known, the TIP4P water model is a good model because it reproduces the water anomaly [16]; however, when the temperature rises gradually away from the stable regime, the SPC/E water model becomes the most convenient, i.e. this water model behaves very well since it allows to observe the stable–unstable transition of the methane hydrates just in the temperature vicinity where the experiment indicates this transition [17].

The coordination number is also used as an indicator when the clathrate begins to lose its stability. This parameter provides the amount of molecules that surround each methane molecule for each equilibrium temperature. For the simplest cage (pentagonal dodecahedron 5^{12}), the number of water molecules that surround the guest molecule is 20 [16]. We assume that a criterion for the hydrate disassociation may be given by determining the linking number between the carbon and oxygen sites corresponding to the methane and water molecules, respectively. Concerning the performance of different water models in the phase diagram line, a comparison was done for models of three, four and five sites. As a result,

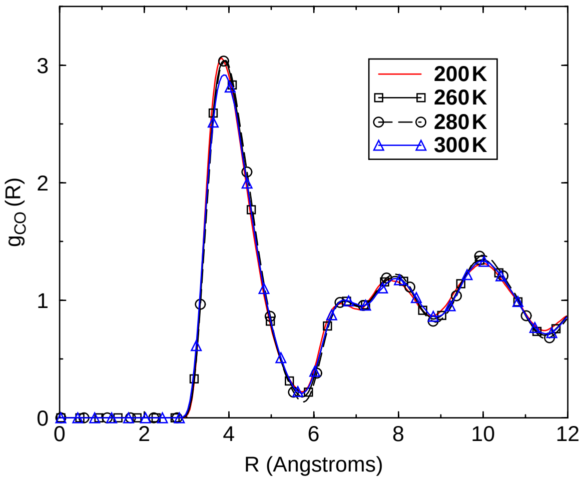

Figure 6. RDF of carbon–oxygen. The water model used was TIP5P, the pressure was fitted at 20 atm and the temperature takes values from $T = 200$ to 300 K. There are no relevant changes in spacial order for the methane hydrate when this water model is used.

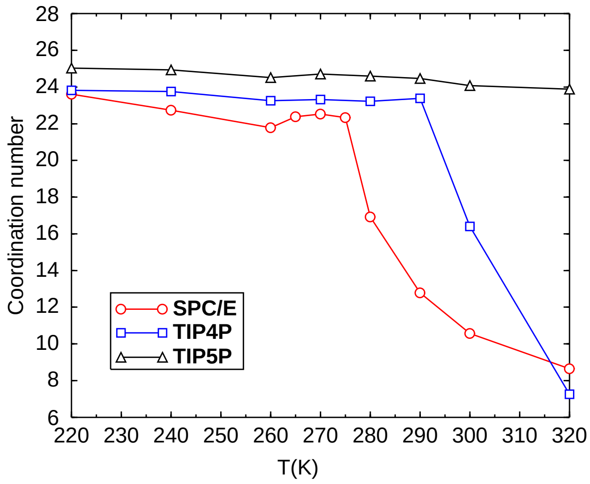

Figure 7. Coordination number as a function of temperature. The open circles correspond to the SPC/E water model results, the open squares and triangles are the results for the TIP4P and TIP5P water model, respectively. The continuous line is included just to guide the eye.

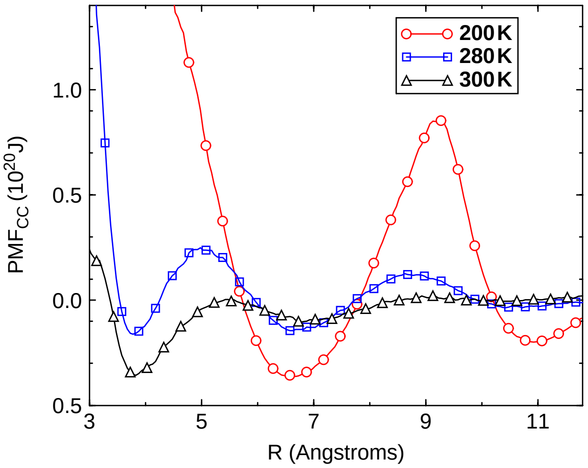

Figure 8. PMF between two methane molecules separated by water. PMFs as a function of temperature are shown. The empty circles correspond to the lower temperature and the empty triangles are the results from the higher temperature.

the rigid non-polarisable SPC/E water model shows the most real perception of the phase system change. It can be observed clearly in Figure 7 that the coordination number of TIP4P and TIP5P water models does not go down from the numeric value of 20 (a criterion established to determine the disassociation of the hydrate), even for higher temperatures above the experimental phase transition (around 268 K at 20 atm) [17]. This is not the case for the SPC/E curve, where we can observe that the performance of this water model yields a coordination number approximated to 17 at 280 K. In the coordination number curve obtained for the SPC/E water model and plotted in Figure 7, a small shoulder can be noticed just before the clathrate disassociation. It may be interpreted as the graphic representation of the metastability of the system exactly in the phase transition.

In Figure 8, the PMF of carbon–carbon association for different temperatures is shown, where two minima can be observed. One of them at short distances (around 6 Å) is the contact minimum and the second one localised at larger distances (around 11.2 Å) is the solvent-separated minimum (at $T = 200$ K). It can be noticed that, as the temperature increases, the energetic barrier diminishes, hence the methane molecules tend to be together. In this same figure, the PMF at a higher temperature shows that the methane compounds lose the stable structural arrangement and they are located in a metastable state allowing the formation of methane aggregates. This kind of behaviour is also observed when the pressure diminishes by fitting the temperature. Actually, Hummer et al. [9] showed similar results for two methane-like particles in water, varying the pressure. In their paper, the authors show that the destabilising effect of temperature increases when pressure diminishes.

4. Conclusions

The performance of the water models of three, four and five sites in the reproduction of structural characteristics of methane hydrate was compared. It was observed that in the stable region, the three models achieve great stability of the system. Nevertheless, the TIP4P and TIP5P water models showed a greater stability that remains beyond the experimental transition line where the system is located in an unstable state. In comparison, the SPC/E model showed a great congruence with the experimental data concerning the disassociation point of the clathrate. The curve for the coordination number showed that methane hydrate is maintained stable beyond the critical temperature region for both the TIP4P and TIP5P water models; thus this parameter gives us complementary information in order to capture the stable–unstable transition of the methane compounds. By analysing the PMF of two methane molecules, the structural changes of the stable clathrate can be observed as well as the temperature dependence. From our results, we may see that the temperature effect yields a situation where the interstitial space between two non-polar molecules is energetically favourable or unfavourable, keeping the pressure at 20 atm. Hence, for higher temperatures, the solvent-separated configuration is more relevant. All these results are in agreement with experimental evidence, mainly, in the experimental temperature region where the critical value is located. Finally, we would like to mention that in the near future, we shall analyse structural changes in methane hydrate placing an external electrical perturbation in the phase transition line and employing the SPC/E water model.

Acknowledgements

D.P. Luis thanks CONACyT-México for financial support through a postgraduate scholarship. J. López-Lemus thanks UAEM and CONACyT for financial support, by grants 2625/2008U and F/52803, respectively. L. Romero-Salazar acknowledges support from CONACyT-México under grant P/49607. The authors acknowledge Laboratorio de Supercomputo at FC-UAEM for technical support.

Notes

1. Email: dluis@itesm.mx
2. Email: mmr@uaemex.mx
3. Email: lors@uaemex.mx

References

[1] B. Chen, I. Ivanov, M.L. Klein, and M. Parrinello, *Hydrogen bonding in water*, Phys. Rev. Lett. 91 (2003), 215503.
[2] E.D. Sloan, *Clathrate Hydrate of Natural Gases*, 2nd ed., Marcel Dekker, New York, NY, 1998.
[3] V.V. Sizov and E.M. Piotrovskaya, *Computer simulation of methane hydrate cage occupancy*, J. Phys. Chem. B 111 (2007), pp. 2886–2890.

[4] L.R. Pratt and D. Chandler, *Theory of the hydrophobic effect*, J. Chem. Phys. 67 (1977), 3683.

[5] J.-L. Li, R. Car, C. Tang, and N.S. Wingreen, *Hydrophobic interaction and hydrogen bond network for a methane pair in liquid water*, Proc. Natl Acad. Sci. 104 (2007), pp. 2626–2630.

[6] D.M. Heyes, *The Liquid State: Applications of Molecular Simulations*, Wiley, Chichester, 1998.

[7] G. Hummer, S. Garde, A.E. García, A. Pohorille, and L.R. Pratt, *An information theory model of hydrophobic interactions*, Proc. Natl Acad. Sci. 93 (1996), pp. 8951–8955.

[8] B.J. Berne, *Inferring the hydrophobic interaction from the properties of neat water*, Proc. Natl Acad. Sci. 93 (1996), pp. 8800–8803.

[9] G. Hummer, S. Garde, A.E. García, M.E. Paulaitis, and L.R. Pratt, *Hydrophobic effects on a molecular scale*, J. Phys. Chem. B 102 (1998), pp. 10469–10482.

[10] G. Hummer, S. Garde, A.E. García, M.E. Paulaitis, and L.R. Pratt, *The pressure dependence of hydrophobic interactions is consistent with the observed pressure denaturation of proteins*, Proc. Natl Acad. Sci. 95 (1998), pp. 1552–1555.

[11] A. Wynveen and F. Bresme, *Interactions of polarizable media in water: A molecular dynamics approach*, J. Chem. Phys. 124 (2006), 104502.

[12] A.D.J. Haymet, *International Conference on Natural Gas Hydrates*, Vol. 715, New York Academy of Sciences, New York, NY, 1994, p. 146.

[13] J.S. Loveday, R.J. Nelmes, D.D. Klung, J.S. Tse, and S. Desgreniers, *Structural systematics in the clathrate hydrates under pressure*, Can. J. Phys. 81 (2003), pp. 539–544.

[14] O. Bonnefoy and J.-M. Herri, *4th International Conference on Gas Hydrates*, hal-00126018 Yokohama, Japan, 2002.

[15] B. Kvamme and T. Kuznetsova, *Hydrate dissociation in chemical potential gradients: Theory and simulations*, Fluid Phase Equilib. 21 (2003), pp. 217–226.

[16] N.J. English and J.M.D. MacElroy, *Atomistic simulations of liquid water using Lekner electrostatics*, Mol. Phys. 100 (2002), pp. 3753–3769.

[17] J.B. Klauda and S.I. Sandler, *A fugacity model for gas hydrate phase equilibria*, Ind. Eng. Chem. Res. 39 (2000), pp. 3377–3386.

[18] J. López-Lemus, G.A. Chapela, and J. Alejandre, *Effect of flexibility on surface tension and coexisting densities of water*, J. Chem. Phys. 128 (2008), 174703.

[19] Z. Cao, J.W. Tester, and B.L. Trout, *Sensitivity analysis of hydrate thermodynamic reference properties using experimental data and* ab initio *methods*, J. Phys. Chem. B 106 (2002), pp. 7681–7687.

[20] M.P. Allen and D.J. Tildesley, *Computer Simulation of Liquids*, Clarendon Press, Oxford, 1987.

[21] D. Frenkel and B. Smit, *Understanding Molecular Simulation: From Algorithms to Applications*, Academic Press, San Diego, CA, 2002.

[22] H.J.C. Berendsen, J.R. Grigera, and T.P. Straatsma, *The missing term in effective pair potentials*, J. Phys. Chem. 91 (1987), pp. 6269–6271.

[23] W.L. Jorgensen and J.D. Madura, *Temperature and size dependence for Monte Carlo simulations of TIP4P water*, Mol. Phys. 56 (1985), pp. 1381–1392.

[24] M.W. Mahoney and W.L. Jorgensen, *A five-site model for liquid water and the reproduction of the density anomaly by rigid, nonpolarizable potential functions*, J. Chem. Phys. 112 (2000), 8910.

[25] Y. Sun, D. Spellmeyer, D.A. Pearlman, and P.J. Kollman, *Simulation of the solvation free energies for methane, ethane, and propane and corresponding amino acid dipeptides: A critical test of the bond-PMF correction, a new set of hydrocarbon parameters, and the gas phase-water hydrophobicity scale*, J. Am. Chem. Soc. 114 (1992), pp. 6798–6801.

[26] P. Ewald, *Die Berechnung optischer und elektrostatischer Gitterpotentiale (Evaluation of optical and electrostatic lattice potentials)*, Ann. Phys. 64 (1921), pp. 253–287.

[27] N. Karasawa and W. Goddard, III, *Acceleration of convergence for lattice sums*, J. Phys. Chem. 93 (1989), pp. 7320–7327.

[28] J. López-Lemus and J. Alejandre, *Thermodynamic and transport properties of simple fluids using lattice sums: Bulk phases and liquid + − vapour interface*, Mol. Phys. 100 (2002), pp. 2983–2992.

[29] J. López-Lemus and J. Alejandre, *Simulation of phase equilibria and interfacial properties of binary mixtures on the liquid-vapour interface using lattice sums*, Mol. Phys. 101 (2003), pp. 743–751.

[30] R. Featherstone, *Rigid Body Dynamics Algorithms*, 2nd ed., Springer-Verlag, New York, NY, 2008.

[31] H.J.C. Berendsen, J.P.M. Postma, W.F. Van Gunsteren, A. Di Nola, and J.R. Haak, *Molecular dynamics with coupling to an external bath*, J. Chem. Phys. 81 (1984), 3684.

[32] R.K. McMullan and G.A. Jeffrey, *Polyhedral clathrate hydrates. IX. Structure of ethylene oxide hydrate*, J. Chem. Phys. 42 (1965), 2725.